Gradual crossover in molecular organization of stable liquid H2O at moderately high pressure and temperature

Koga, Yoshikata; Westh, Peter; Yoshida, Koh; Inaba, Akira; Nakazawa, Yasuhiro

Gradual crossover in molecular organization of stable liquid H2O at moderately high pressure and temperature

Yoshikata Koga, Peter Westh, Koh Yoshida, Akira Inaba, and Yasuhiro Nakazawa

---

Gradual crossover in molecular organization of stable liquid H$_2$O at moderately high pressure and temperature

Yoshikata Koga,[1,a] Peter Westh,[2] Koh Yoshida,[3] Akira Inaba,[3] and Yasuhiro Nakazawa[3]

[1]*Department of Chemistry, The University of British, Columbia, Vancouver, BC, Canada V6T 1Z1, and Suitekijuku, Vancouver, BC, Canada V6R 2P5*
[2]*NSM, Research Unit for Functional Biomaterials, Roskilde University, Roskilde, Denmark DK-4000*
[3]*Research Center for Structural Thermodynamics, Osaka University, Toyonaka, Osaka, Japan 560-0043*

Using the literature raw data of the speed of sound and the specific volume, the isothermal compressibility, κ_T, a second derivative thermodynamic quantity of G, was evaluated for liquid H$_2$O in the pressure range up to 350 MPa and the temperature to 50 °C. We then obtained its pressure derivative, dκ_T/dp, a third derivative numerically without using a fitting function to the κ_T data. On taking yet another p-derivative at a fixed T graphically without resorting to any fitting function, the resulting d$^2\kappa_T$/dp^2, a fourth derivative, showed a weak but clear step anomaly, with the onset of the step named point X and its end point Y. In analogy with another third and fourth derivative pair in binary aqueous solutions of glycerol, dα_p/dx_{Gly} and d$^2\alpha_p$/dx_{Gly}^2, at 0.1 MPa (α_p is the thermal expansivity and x_{Gly} the mole fraction of solute glycerol) in our recent publication [*J. Solution Chem.* **43**, 663-674 (2014); **DOI**:10.1007/s10953-013-0122-7], we argue that there is a gradual crossover in the molecular organization of pure H$_2$O from a low to a high p-regions starting at point X and ending at Y at a fixed T. The crossover takes place gradually spanning for about 100 MPa at a fixed temperature. The extrapolated temperature to zero p seems to be about 70 – 80 °C for points X and 90 – 110 °C for Y. Furthermore, the mid-points of X and Y seem to extrapolate to the triple point of liquid, ice Ih and ice III. Recalling that the zero x_{Gly} extrapolation of point X and Y for binary aqueous glycerol at 0.1 MPa gives about the same T values respectively, we suggest that at zero pressure the region below about 70 °C the hydrogen bond network is bond-percolated, while above about 90 °C there is no hydrogen bond network. Implication of these findings is discussed. © *2014 Author(s). All article content, except where otherwise noted, is licensed under a Creative Commons Attribution 3.0 Unported License.* [http://dx.doi.org/10.1063/1.4895536]

I. INTRODUCTION

While "thermodynamics" of super-cooled water has been extensively studied of late,[1,2] we limit ourselves here to the stable liquid phase in the moderately high pressure and temperature region covered by the p-T range shown in Fig. 1. In the stable phase region, the proper thermodynamics is applicable. The filled black circles in Fig. 1 are the phase boundaries determined by Bridgeman,[3] and Kell and Whalley.[4] The densities of ice (g cm^{-3}) that forms coexisting with liquid are given in the bracket in the figure. It is generally accepted that the molecular organization of liquid H$_2$O has some reminiscence to the structure of the solid that share the solid-liquid boundary. Okhulikov et al.[5]

---

[a]Correspondence should be addressed to this author. Electronic address: koga@chem.ubc.ca
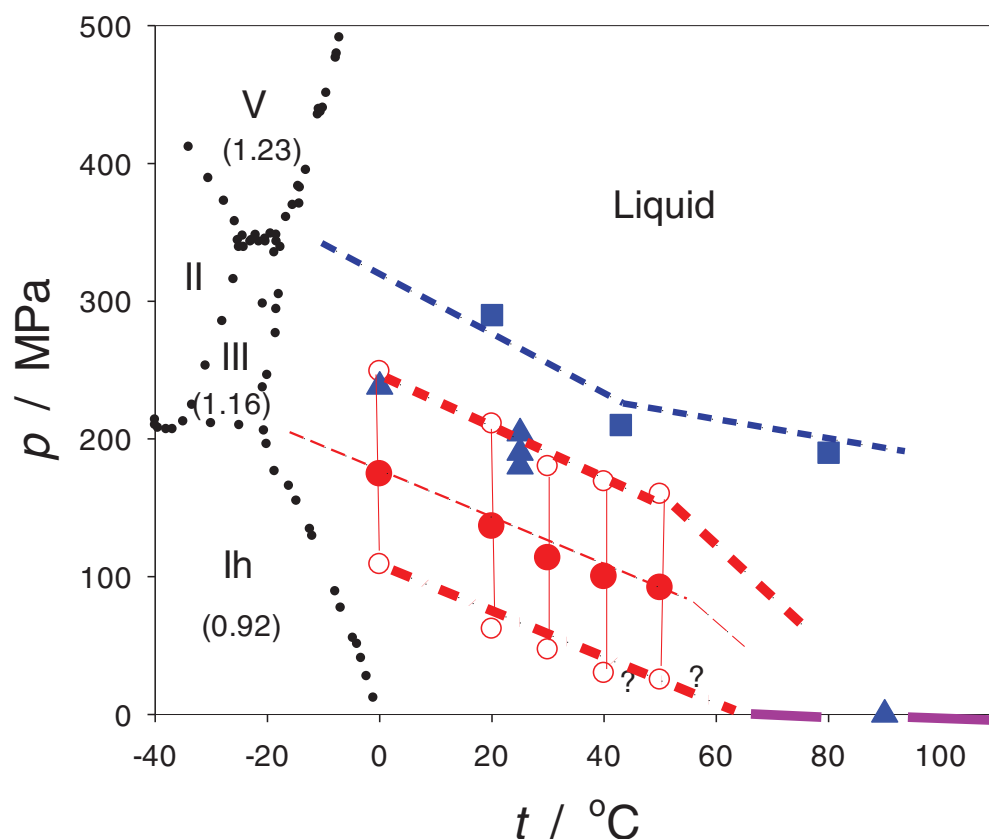
4, 097116-1 © Author(s) 2014

FIG. 1. Phase diagram of water, and regions of liquid water with different molecular organization. Filled black circles; solid-liquid and solid-solid phase boundaries.[3,4] Blue broken line; boundary between "high-" and "low-density" liquid.[6] Blue filled square; from Brillouin scattering.[7] Blue filled triangle; from femtosecond pump-probe spectroscopy.[8] Red hollow circles, red filled circles, red lines and purple lines; this work. For the thick dot-dash line for point X, thick broken line for point Y, and thin broken line for mid-points of X and Y, see text for details.

fit the pair correlation function determined by x-ray scattering measurements to the composition weighted sum of those of a Lenard-Jones fluid, ice Ih, III, V and VI. They found that the dominant species below 200 MPa is that of ice Ih, while the contribution from that of ice III has its maximum contribution at about 300 MPa, and at about 450 MPa for ice V structure. As is obvious from Fig. 1, these pressure values fall within the appropriate range corresponding to the respective forms of ice that share the solid-liquid boundary. Saitta and Datchi,[6] by using MD simulation, identified that the "high density water" has a local structure precursory to ice VI or ice VII, and showed the boundary to the "low density liquid" as sketched roughly by blue broken line in Fig. 1. Li *et al.*[7] showed that the logarithm of bulk modulus calculated from the observed split of Brillouin scattering and the literature density data, against the logarithm of density showed a break in slope, the loci of which are plotted as filled blue squares in Fig. 1. These points seem to be coincidental with the blue broken line.[6] Recently, by femtosecond pump probe mid-infrared spectroscopy, Fanetti *et al.*[8] observed breaks in the slope of *p*-evolution of the vibrational line width and related dynamics and anisotropy decay. With the aid of MD simulation, they interpreted such breaks in slope to show the boundary between a "low-" and a "high-density" liquid H_2O. They are also plotted in Fig. 1 as blue triangles.

Here, in order to examine a possible existence of multi-kinds of liquid water within the single stable phase, we apply a differential approach in solution thermodynamics, which we previously introduced and applied in studies of aqueous solutions of non-electrolytes at the ambient pressure.[9–11] The principle of the methodology is based on general observation that the higher the order of derivative, the more sensitive it is to subtle changes in molecular organization. Thus, as long as

the very precise experimental data are available, higher derivatives provide deeper insight. In the experimentalist's favourite (p, T, n_i) variable system, Gibbs' energy, G, dictates the stability of an equilibrium system. Its T derivative once will separate H and S out of G. Further differentiation with respect to T results in C_p, a second derivative, that is proportional to the mean square fluctuation in H or S. In obtaining higher order derivative quantities, direct experimental determination would be the best. At this point in time, the second derivative quantities can be commonly measured; response functions for example. We directly measured the excess partial molar enthalpy of a solute B, H_B^E, another second derivative of G. Following our principle, we raised the order of derivative by calculating a third derivative using the H_B^E data. We do this without resorting to any fitting function, as that would tend to mask a slight anomalous behaviour in raw, a lower degree of derivative data, which leads to a devastating loss of detail when differentiated. We thus graphically or numerically (if the raw data are of high quality and obtained in a small enough increment) determined the next derivative with respect to the molar amount of B, n_B, resulting in the B-B enthalpic interaction, H_{BB}^E, a 3rd derivative.[9–12] For a favourable case, we were able to develop a differential pressure perturbation calorimeter and measured the partial molar entropy-volume cross fluctuation density of solute B, $^{SV}\delta_B$, a 3rd derivative of G, directly[13] and then graphically determine a 4th derivative quantity, $^{SV}\delta_{BB}$, again without relying on any fitting function.[14] We found this approach was effective in elucidating the detailed molecular level scenario of mixing. For example, the third derivative quantities showed an anomaly or a singularity which defined the boundary of two qualitatively different mixing schemes.[9–12] See the Appendix. As mentioned above, we apply this differential methodology on pure H_2O in the current work and see if there is any singular behaviour in the third derivative quantities for pure liquid water at moderately high pressure-temperature region, to investigate a possible crossover of molecular organization in pure H_2O, such as "high-" and "low-density liquids".

II. DATA TREATMENT

For water, there are voluminous thermodynamic data available in literature, for density (1st derivative) and response functions (2nd derivative). But all of these precise measurements were always smoothened by curve-fitting to analytic functions with a variety of complexity. Our purpose here is to seek anomalous behaviours in the third derivatives, and a subtle wiggle at 1st or 2nd derivative level would be masked when expressed by an analytic function. Fortunately, two papers were published recently that contain the raw data of the speed of sound, u,[15] and the specific volume, v,[16] in H_2O in the pressure and temperature range similar to that covered in Fig. 1. The former u measurements were done at 273.21, 293.16, 303.14, 313.16, and 323.16 K within $\pm$ 0.015 K. For the v values, on the other hand, the temperature was controlled better than 0.1 K at the average 273.6, 293.4, 303.5, 313.4 and 323. 3 K. For the present data analysis, we ignore about 0.3 K difference in T between the two sets of u and v data and consider the common temperatures of 273, 293, 303, 313 and 323 K. For the pressures, while both covering from 0.1 to 350 MPa, the respective increments are not identical. The values of v were taken at about 0.1, 70, 100, 150, 200, 250, 300, and 350 MPa within $\pm$ 0.005 MPa, while those of u at 1, 5, 10, 15, 25, 50, 75, 100, 125, 150, 175, 200, 225, 250, 275, 300, and 350 MPa within $\pm$ 0.005 MPa. The uncertainty in the results of u is given as 0.04 %[15] and at worst 3×10^{-4} cm^3 g^{-1}, and 0.03 % for the v data.[16] Since the v values are determined at the pressures different from those for the u values, particularly so for the range $p < 70$ MPa, we have to interpolate the values of v at the values of p of the u measurement without relying on curve fitting procedure. We devised a second order polynomial function so that the residual from the measured value of v becomes about a few times of the total uncertainty. We then interpolated the residual values linearly and recalculated v at the same value of p for the u data.[15] In this way the value of v is obtained with five significant figures without resorting to a fitting function. With these values of u and v at given values of T and p, the isentropic compressibility, κ_S, was calculated as,

$$\kappa_S = v/u^2, \tag{1}$$

within $\pm$ 0.05 %, with four significant figures, without resorting to any fitting function. We then converted to the isothermal compressibility, κ_T, by the following equation,

$$\kappa_T = \kappa_S + Tv(\alpha_P)^2/c_p, \tag{2}$$

where α_p is isobaric thermal expansivity and c_p specific heat capacity. As is evident in Table S1, Supplementary Material,[30] the correction term, the second term of the right of eq. (2), is the smallest at low T and p; with 0 % at 273 K and 1 MPa, and increases to about 7 % at 323K and 350 MPa. Therefore, the anomalous behaviour in the correction term, if any, gives little effect on the singularity in the κ_T data due to the dominance of the first term. Hence, we evaluated the value of α_p from the fitted function given by Ter Minassian *et al.*,[17] and the thermodynamically integrated value of molar heat capacity, C_p, were used to interpolate the necessary value of the specific heat capacity, c_p, in eq. (2). The process of these calculations are shown in the second sheet, "kappaT", of Table S1.[30]

III. RESULTS AND DISCUSSION

Table S1 of the supplementary material[30] shows κ_T vs. p at given temperatures. κ_T is proportional to the mean square volume fluctuation density.[18,28] For pure liquid H_2O, κ_T, or the volume fluctuation decreases as p increases as shown in Fig. 2. This was attributed to the decrease in putative formation of ice-like patches due to Le Chatelier principle rather than direct reduction of the hydrogen bond probability by pressure increase.[18,28] Fig. 2 does not seem to show any anomalous behaviour, at the second derivative level. However, the κ_T data at hand are the closest to the proper experimental raw data of a second derivative in the Gibbs variable system.[29] We therefore seek first any singular behaviour in its p-derivative, a third derivative. Given the limited p intervals, we calculate $d\kappa_T/dp$ numerically with T constant using adjacent data points. Namely, we approximate the derivative, $(\partial\kappa_T/\partial p)_T$, as the tangent of the code connecting two adjacent data points with constant T. Judging from a weak curvature of κ_T against p in Fig. 2, the above approximation should be acceptable. The results are shown in the 3$^{\text{rd}}$ sheet, "p-derivative of kappaT" of Table S1,[30] and plotted in Fig. 3; for all temperatures in Fig. 3(a) and for 293 K in Fig. 3(b). The p-dependence of $d\kappa_T/dp$, a third derivative, has an almost linear portion at low p, particularly for 273 and 293 K, as evident in Fig. 3(a) and 3(b). Namely, the effect of p on the volume fluctuation stays almost linear up to some value of p and then such effect starts to fade away gradually.

We now recall our earlier studies of aqueous solutions of glycerol (Gly) at the ambient pressure. As described in the Appendix, the behaviour of x_{Gly}-effect on another third derivative, $^{SV}\delta_{\text{Gly}}$ (Fig. 6(a) in the Appendix), appears similar to the present p-effect on $d\kappa_T/dp$ in Fig. 3 except for the ordinate direction. $^{SV}\delta_{\text{Gly}}$ is the partial molar entropy-volume cross fluctuation density of glycerol (Gly) in Gly - H_2O determined directly at 15 °C, and x_{Gly} is the mole fraction of Gly.[19] This type of anomaly, the bend type, is typical for hydrophilic solutes, and is not as conspicuous as the peak type for hydrophobic solutes. See the Appendix for details. Hence locating anomalous points, if any, is problematic, in comparison with the case for a hydrophobic solute. For such a case, we take one more derivative with respect to the independent variable graphically. As discussed in the Appendix, if there is a bend type anomaly in a third derivative, then the fourth derivative must show a step, its onset, X, being the point where the crossover of mixing scheme starts and the end of the step, Y, the end of the crossover process.

We apply this technique to the data shown in Fig. 3, to seek if there is indeed a bend-type anomaly in $d\kappa_T/dp$, a third derivative, for pure water. Since the values of $d\kappa_T/dp$ are calculated numerically using the adjacent data points from the direct experimental determination, and since the resulting data of $d\kappa_T/dp$ appear smooth except for the very low pressure region, we should be allowed to take the next derivative graphically. We draw a smooth curve through all the data points with aid of a flexible ruler. We then read the data off the smooth curve with four significant figures at the interval of $\delta p = 20$ MPa and approximated the slope of the small code to that of the tangent, $d^2\kappa_T/dp^2$, at the mid-point. The appropriateness of such approximation was discussed at some length earlier.[20] Results are plotted in Fig. 4. It is evident that there is a weak but clear step type anomaly, which reflects a bend-type anomaly in $d\kappa_T/dp$, a third derivative quantity. In analogy of our findings in binary aqueous solutions, it may be safe to conclude that in pure liquid H_2O there is some change
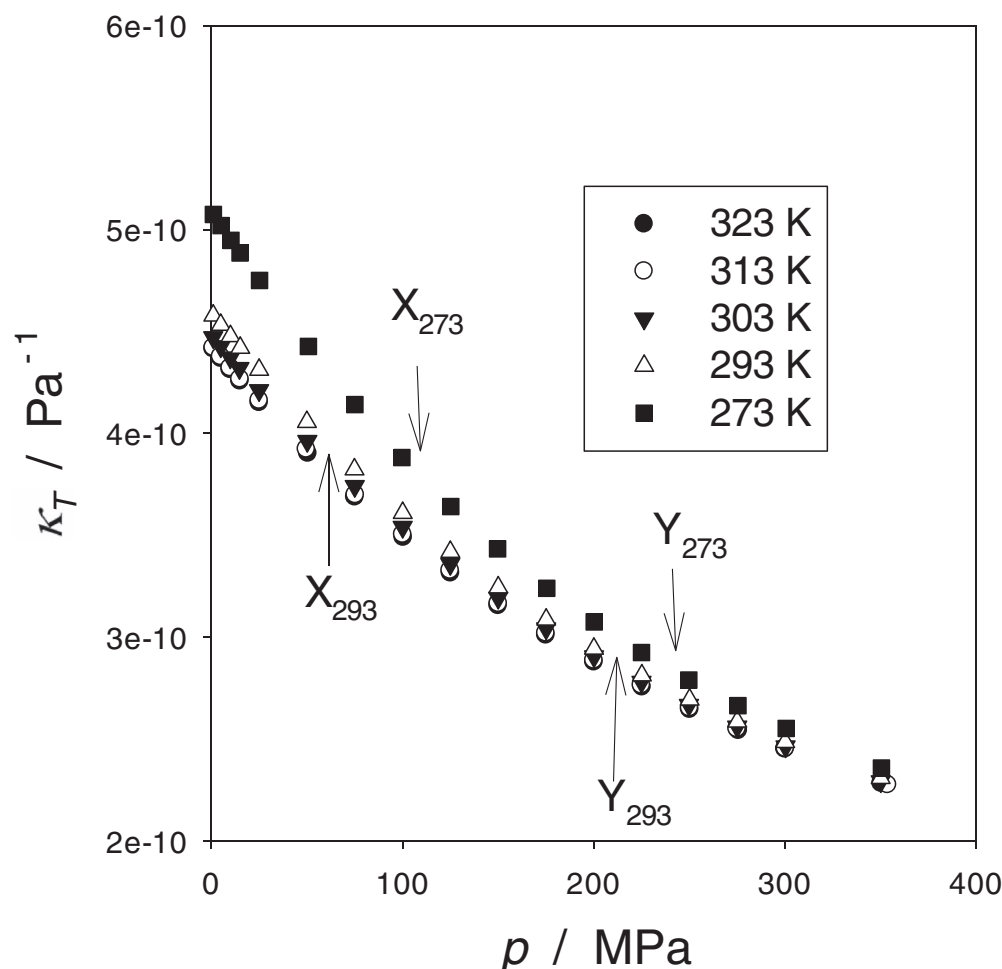
FIG. 2. The calculated κ_T vs. p for liquid H_2O. X_{273} etc. mark the point X and Y at 273 K etc., the onset and the end point of gradual transition, determined from the step anomalies in the double p derivative of κ_T. See Fig. 4. These anomalous points in the higher order derivative are not conspicuous in the behaviour of κ_T, the second derivative of G.

in the molecular organization of H_2O. Namely, there is one kind of molecular organization in liquid H_2O below point X, and another kind above point Y. It is a rather smooth crossover starting at point X, shown in Fig. 4, and ends at point Y. They are plotted as red hollow circles in Fig. 1. For 313 and 323 K, the point X is not clearly defined in Fig. 4(b). They must be at small p, less than 30 MPa, if present.

As is clear from Fig. 1, the boundary zone from point X to Y slants with a negative slope of dp/dT. While the present gradual cross over is not a "phase transition", for it is associated with a weak step anomaly in the fourth derivative quantity, $d^2\kappa_T/dp^2$. Thus, the Clapeyron relation does not hold for the slope of the boundary. Nevertheless, it is interesting to note that the boundary zone on crossing from a "low density" to a "high density region" shows a negative dp/dT, just as the phase boundary crossing from ice Ih to liquid water. In this connection, it seems worthy of noting that Kawamoto *et al.*[31] followed the Raman OH stretch frequency shift of liquid H_2O by increasing p with a fixed T. They found a clear break in its p-dependence, and interpreted among other possibilities it as the crossover from the "low density" to the "high density liquid" whose structures were studied by neutron diffraction by Soper and Ricci,[32] since at −5 °C the boundary values coincide with each other. Although they are about 200 MPa higher than the present boundary zone shown in Fig. 1, Kawamoto *et al.* found that on increasing T the p-loci of the break increases, i. e. $dp/dT > 0$.[31] As discussed below, there could be another crossover in the molecular organization
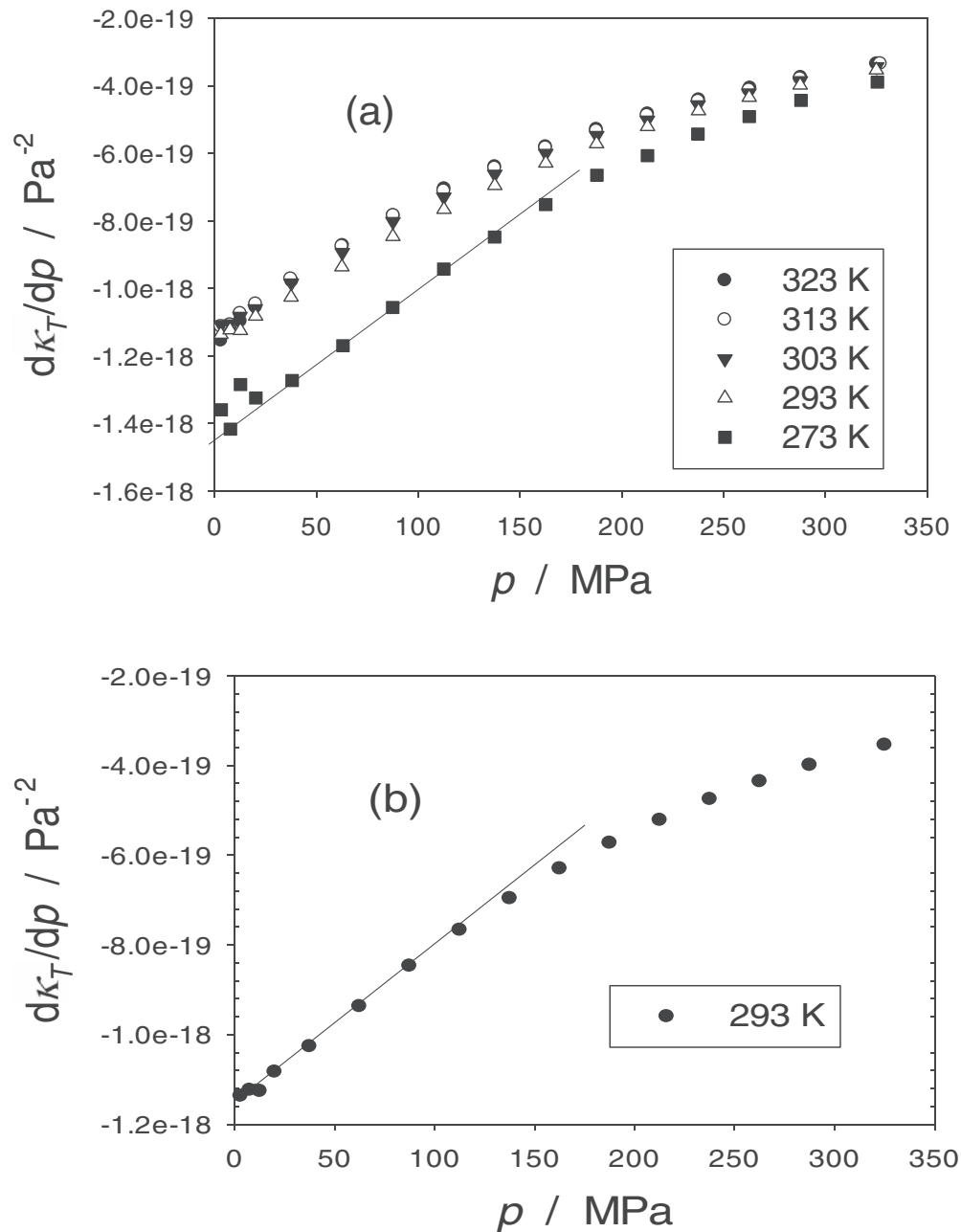
FIG. 3. (a). The *p*-derivative of κ_T for pure liquid H_2O. The straight line is for a guide for eyes. See text. (b) The *p*-derivative of κ_T for pure liquid H_2O at 293 K. The straight line is for a guide for eyes. See text.

of stable liquid water. Whether such an extra boundary exists or not, and in which way it slants are yet to be elucidated.

Going back to Fig. 1, the mid-points between point X and Y are plotted as red filled circles. We note in Fig. 1 that the extrapolation of points X and Y (red hollow circles) to zero (0.1 MPa) pressure seems to aim at 70–80 °C for X and 90–110 °C for Y. Furthermore, the mid-points seem to extrapolate in the other direction to the triple point of liquid, ice Ih and ice III.

We recall our studies on binary aqueous solutions of hydrophobes and hydrophiles, in which we plotted the loci of point X against temperature in binary aqueous solutions at 0.1 MPa. For a single solute, the points X for a variety of 3rd derivatives converge into a single sigmoidal curve
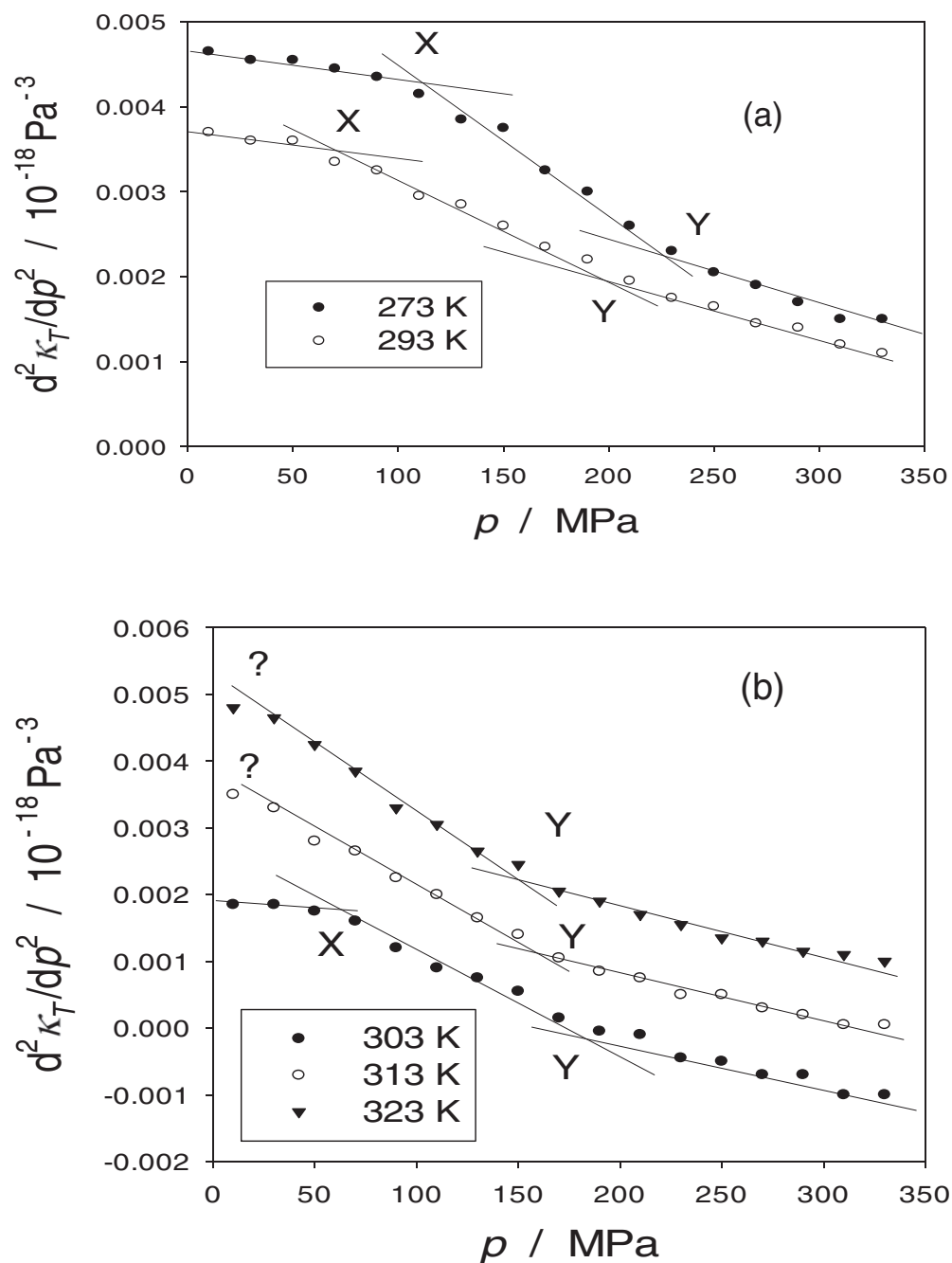
FIG. 4. (a) The double p-derivative of κ_T for pure liquid H_2O at 273 and 293 K. Step anomalies are evident. Point X is the onset and Y the end of gradual crossover. See text. (b) The double p-derivative of κ_T for pure liquid H_2O at 303, 313 and 323 K. Step anomalies are evident. Point X is the onset and Y the end of gradual crossover. See text.

that we call the Koga line.[12, 19] The collection of the Koga lines including hydrophilic Gly seem to extrapolate to the infinite dilution at the unique value of about 70 – 80 ºC, independent of the identity and the class of solute.[19] Since in our earlier studies point Y has not been paid attention, in Fig. 5 we re-plotted the loci of point X for a few selected solutes, for which those of point Y are also available. The extrapolated value of point Y seem to be about 90 – 110 ºC, taking into account of the original sigmoidal curvature. These possible end point temperature ranges of point X and Y in Fig. 5 are also shown by purple lines on the abscissa of Fig. 1.
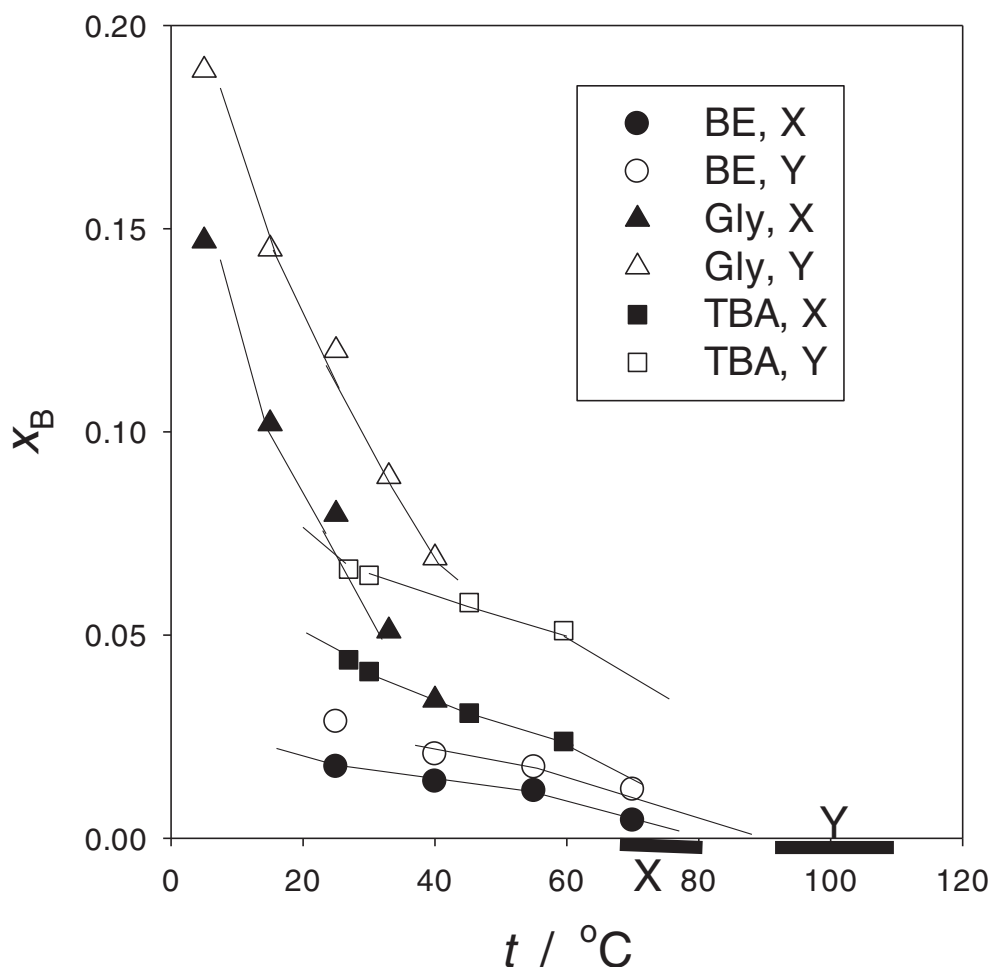
FIG. 5. The temperature loci of point X and Y for aqueous solutions of a selected solutes, B, at the ambient pressure. The loci of point X (filled symbols) tend to extrapolate to the infinite dilution of the mole fraction, x_B, at about 70 to 80 °C, and Y (hollow symbols) at about 90 to 110 °C. These regions are indicated by two thick lines on the t axis. BE; 2-butoxyethanol.[19] Gly; glycerol.[19] TBA; tert-butanol.[28]

The implication of Fig. 1 is profound. It is clear that there is a gradual boundary in stable liquid H_2O region spreading more than 100 MPa for a fixed T, and about 100 °C for a given p. An interesting point to note is that the blue triangle plots from femto-second pump-probe spectroscopy seem to coincide with the present point Y.[8] The blue triangle plot at 90 °C on the abscissa is the point at which the authors observe their "high density water" only.[8] This could mean that the thick red broken line for point Y may bend down so that it points to below 90 °C on the abscissa. It would force the thin red broken line, a nominal boundary, to bend down also. The degree of which is yet to be determined.

It is remarkable that the zero pressure ends of point X and Y for pure water match the infinite dilution ends of the Koga lines and the points Y, the thick purple lines on the abscissa in Fig. 1. In our earlier thermodynamic studies on aqueous solutions of non-electrolytes, we suggested that the Koga lines separate the mole fraction – temperature field into two, the low mole fraction and temperature side of which is where the integrity of liquid H_2O is retained while accommodating dilute solutes in a specific manner depending on the nature of solute; hydrophobic or hydrophilic. The other side of the collections of point Y are regions where a physical mixture of two kinds of clusters exist, one rich in H_2O and the other in solute molecules, i. e. the hydrogen bond percolation no longer exists. We noted following the site-correlated percolation model by Stanley *et al.*[21] that the important factor across the Koga line and point Y's is the loss of hydrogen bond percolation.[10–12]

The coincidence of the temperature range at zero pressure for pure H_2O and at the infinite dilution of aqueous solutions at the ambient pressure suggests that the region below the thick red dot-dash boundary in Fig. 1 is also the region in which the hydrogen bond percolation remains intact while local hydrogen bonds are fleetingly forming and breaking. This indeed shows a resemblance to the known crystal structure of ice Ih. Above the thick red broken line, on the other hand, liquid H_2O loses its hydrogen bond connectivity. The structure of ice III is known to be tetragonal. While the first neighbour distance is about the same as in Ih, the non-hydrogen bonded neighbour is much shorter, about 3.6 Å in comparison with that of Ih 4.50 Å, that explains the increase in density from 0.92 to 1.16 g cm^{-3}.[22] This should be accompanied by a large distortion of hydrogen bonds; with the O-O-O angle of 143º instead of 109.3º of Ih.[22,23] A similar structure is known for ice V with the inter O atom angles taking the values of 89.5 º and 128. 1º.[24] It is also known that H-O-H angle in ice Ih is 107 ± 1º,[25] and 106.3º ± 4.9º in liquid.[26] If the liquid above the Y-boundary has some reminiscence to ice III or V, such a large bending angle could indicate broken hydrogen bonds in liquid. Such an increase in density from the "low density" to the "high density liquid" was pointed out by neutron diffraction studies.[32,33] Thus the hydrogen bonds of the liquid in this region could have lost hydrogen bond percolation. We may suggest to call liquid H_2O in the region below the X-boundary in Fig. 1 "liquid (Ih)" rather than "low-density liquid". Even in the range between X and Y, the bottom half may be closer to liquid (Ih), since the thin red broken line points to the triple point of liquid - ice Ih - ice (III). We stress, however, that "liquid (Ih)" is not a separate phase. The anomaly in the crossover to the higher pressure modification is evident only in the third derivative, and more clearly in the fourth derivative, in contrast to phase transitions accompanied by anomalies in the second derivatives. Furthermore, the boundary from point X to Y is wide, spanning about 100 MPa at a fixed temperature; about the same size of ice III region. Hence, the molecular organization of H_2O above the Y-boundary could resemble the structure of ice III or ice V, not inconsistent with the neutron scattering studies.[32,33] Still, the fact that the blue boundary by MD simulation[6] and Brillouin scattering observation[7] seems to head to another triple point of liquid, ice III and ice V could be important results. Further investigation of this "high density liquid" is required to elucidate whether what might be called as "liquid (III)" and "liquid (V)" exist separately or not.

ACKNOWLEDGMENT

Appendix

Fig. 6(a) shows a third derivative quantity, $^{SV}\delta_{Gly}$, the partial molar entropy-volume cross fluctuation density of solute glycerol (Gly) in aqueous solution of Gly at 15 ºC and the ambient pressure. The data were determined directly by the differential pressure perturbation calorimeter.[19] $^{SV}\delta_{Gly}$ is defined as,

$$^{SV}\delta_{Gly} \equiv N(\delta^{SV}\delta/\delta n_{Gly}) = (1 - x_{Gly})(\delta^{SV}\delta/\delta x_{Gly}),$$

$$^{SV}\delta \equiv <(S - <S>)(V - <V>)>/<V> = T\alpha_p,$$

where n_{Gly} is the molar amount of Gly in aqueous solution of Gly, the total molar amount of which is N. x_{Gly} is the mole fraction of Gly in solution, and α_p is the isobaric thermal expansivity. $<>$ signifies the ensemble average of the quantity inside. The figure shows a bend-type anomaly in x_{Gly} dependence pattern.[19] This behaviour is typical for a hydrophilic solute, Gly being an example, and contrasts sharply to that for a hydrophobe. Fig. 6(b) shows the same quantity for a hydrophobic solute 1-propanol at 25 ºC.[12] Among other experimental observations together with the findings
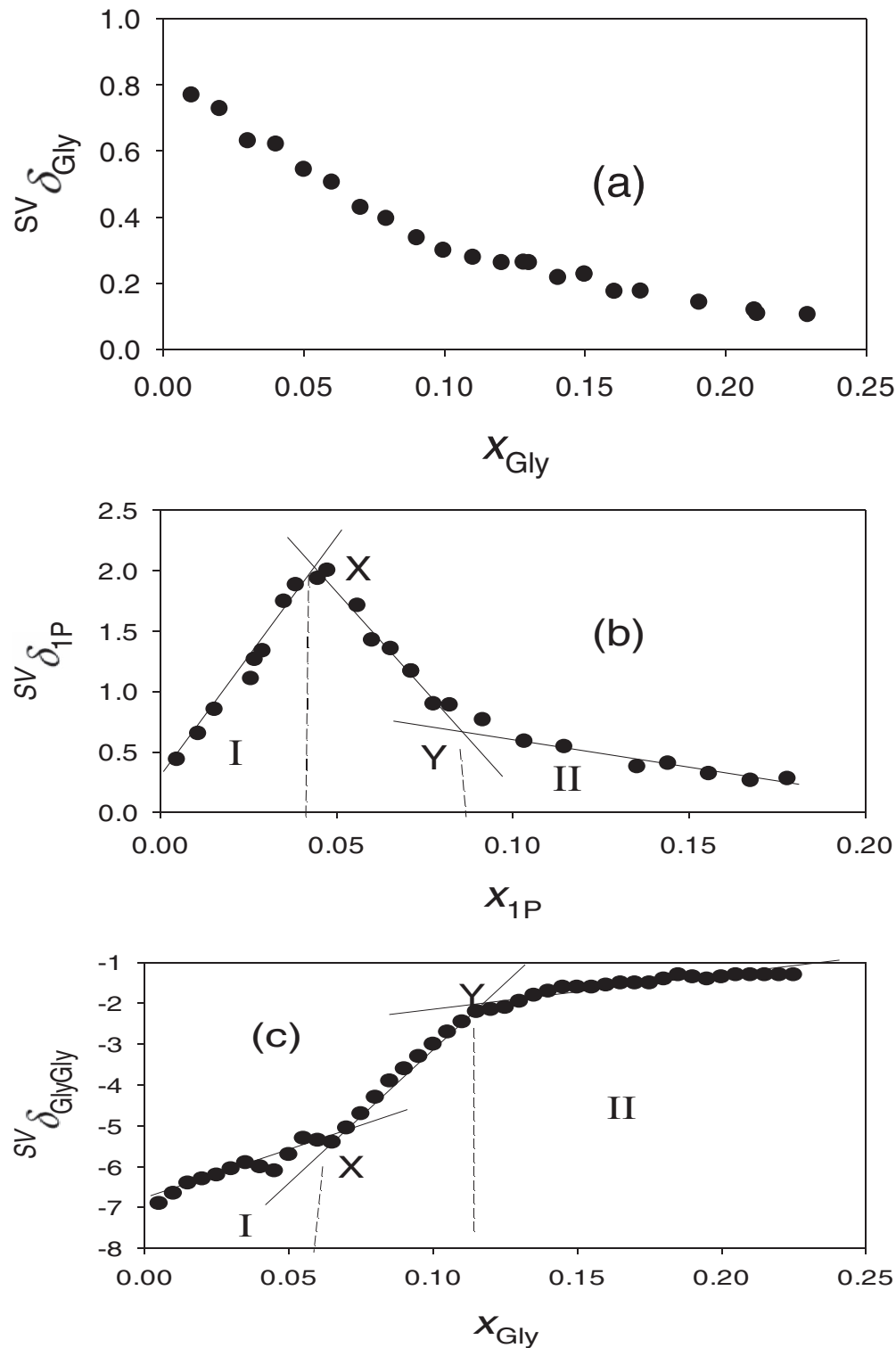
FIG. 6. (a) The partial molar entropy-volume cross fluctuation density of glycerol (Gly), $^{SV}\delta_{Gly}$, a third derivative in the binary aqueous Gly at 15 °C determined directly.[19] (b) The partial molar entropy-volume cross fluctuation density of 1-propanol (1P), $^{SV}\delta_{1P}$, a third derivative in the binary aqueous 1P at 25 °C.[12] (c) The double x_{Gly} derivative of $^{SV}\delta$, $^{SV}\delta_{GlyGly}$, for aqueous solution of glycerol (Gly) at 15 °C.[14] A step anomaly is evident, which assures the bend anomaly in $^{SV}\delta_{Gly}$ shown in Fig. 6(a). From this, pint X and Y can be determined with confidence.

shown in Fig. 6(a) and 6(b), we suggested that for both hydrophobic and hydrophilic solutes, their aqueous solutions have in general three distinctive mole fraction regions in each of which the mixing scheme, the molecular level scenario of mixing, is qualitatively different from those in the other regions. In the most H_2O-rich region, where what we call Mixing Scheme I is operative, the molecular organization of liquid water is modified somewhat, but the general integrity of liquid H_2O is retained. Namely, the hydrogen bond network remains bond-percolated. The details of how H_2O is modified depend crucially on the nature of solute. Indeed, a sharp contrast within Mixing Scheme I up to point X is shown in Fig. 6(a) and 6(b), which reflects the detailed difference between hydrophobic and hydrophilic solutes. This was discussed extensively earlier.[10–12,27] The Mixing Scheme II is where the H_2O-rich and the solute-rich clusters physically mix and the hydrogen bond percolation is lost completely at point Y. The narrow region from point X to Y is interpreted as a transient region. We note that the behaviour of third derivatives in Mixing Scheme II are similar in terms of their values and mole fraction dependences.[10–12,27] As is clear from Fig. 6, the points X and Y for hydrophiles (Fig. 6(a)) are not as conspicuous as those for hydrophobes (Fig. 6(b)). To locate these anomalous points, we take one more derivative with respect to the active variable, in this case x_{Gly}, graphically without resorting to a fitting function. Since $^{SV}\delta_{Gly}$ is determined experimentally the graphical differentiation should be acceptable. Fig. 6(c) shows the resulting 4th derivative quantity.[14] We now clearly identify point X and Y in Fig. 6(a) by the onset and the end points of the step anomalies in Fig. 6(c). This technique was used in the main text to obtain Fig. 4.

[1] V. Holten, C. E. Bertrand, M. A. Anisimov, and J. V. Sengers, J. Chem. Phys. **136**, 094507 (2012).

[2] H. Tanaka, Eur. Phys. J. **E35.10**, 1 (2012).

[3] P. W. Bridgeman, Proc. Am. Acad. Arts Sci. **47**, 441 (1912).

[4] G. S. Kell and E. Whalley, J. Chem. Phys. **48**, 2359 (1968).

[5] A. V. Okhulikov, Y. N. Demianets, and Y. E. Gorbaty, J. Chem. Phys. **100**, 1578 (1994).

[6] A. M. Saitta and F. Datchi, Phys. Rev. **67**, 020201(R) (1 (2003).

[7] F. Li, Q. Cui, Z. He, J. Zhang, Q. Zhou, G. Zou, and S. Sasaki, J. Chem. Phys. **123**, 174511 (1 (2005).

[8] S. Fanetti, A. Lapini, M. Pagliai, M. Citroni, M. Di Donato, S. Scandolo, R. Righini, and R. Bini, J. Phys. Chenistry Lett. (2014).

[9] Y. Koga, *Solution Thermodynamics and Its Application to Aqueous Solutions: A Differential Approach (ALL)* (Elsevier B. V., Amsterdam, 2007), pp. 1–296.

[10] Y. Koga, J. Phys. Chem. **100**, 5172 (1996).

[11] Y. Koga, Phys. Chem. Chem. Phys. **15**, 14548 (2013).

[12] Y. Koga, *Solution Thermodynamics and Its Application to Aqueous Solutions: A Differential Approach (V)* (Elsevier B. V., Amsterdam, 2007), pp. 89–150.

[13] K. Yoshida, S. Baluja, A. Inaba, K. Tozaki, and Y. Koga, J. Solution Chem. **40**, 1271 (2011).

[14] K. Yoshida, S. Baluja, A. Inaba, and Y. Koga, J. Chem. Phys. **134**, 214502 (2011).

[15] C.-W. Lin and J. P. M. Trusler, J. Chem. Phys. **136**, 094511(1 (2012).

[16] B. Guignon, C. Aparicio, and P. D. Sanz, J. Chem. Eng. Data **55**, 3338 (2010).

[17] L. Ter Minassian, P. Pruzan, and A. Soulard, J. Chem. Phys. **75**, 3064 (1981).

[18] Y. Koga, *Solution Thermodynamics and Its Application to Aqueous Solutions: A Differential Approach (IV)* (2007), pp. 69–86.

[19] K. Yoshida, A. Inaba, and Y. Koga, J. Solution Chem. **43**, 663 (2014).

[20] M. T. Parsons, P. Westh, J. V. Davies, C. Trandum, E. C. H. To, W. M. Chiang, E. G. M. Yee, and Y. Koga, J. Solution Chem. **30**, 1007 (2001).

[21] H. E. Stanley and J. Teixeira, J. Chem. Phys. **73**, 3404 (1980).

[22] B. Kamb and A. Prakash, Acta Crystographica **B24**, 1317 (1968).

[23] K. Suzuki, *Water and Aqueous Solutions* (Kyouritsu, Tokyo, 1982), p. 55.

[24] B. Kamb, A. Prakash, and C. Knobler, Acta Crystographica **22**, 706.

[25] W. F. Kuhs and M. S. Lehmann, in *Water Sci. Rev.*, edited by F. Franks (Cambridge University, Cambridge, 1986), p. 1.

[26] G. S. Fanourgakis and S. S. Xantheas, J. Chem. Phys. **124**, 174504 (2006).

[27] Y. Koga, *Solution Thermodynamics and Its Application to Aqueous Solutions: A Differential Approach (VI)* (Elsevier B. V., Amsterdam, 2007), pp. 151–173.

[28] Y. Koga, Can. J. Chem. **66**, 1187 (1988).

[29] Of course, κ_s itself is a 2nd derivative and can be used to seek anomalies in its p-derivative. However, in the present data analysis in the (p, T) variable system, it is not proper in that keeping S constant forces both δp and δT nonzero in taking the derivative $(\partial V/\partial p)_S$.

[30] See Supplementary Material Document No. http://dx.doi.org/10.1063/1.4895536 for calculation of κ_T, and its p- and double p-derivatives.

[31] T. Kawamoto, S. Ochiai, and H. Kagi, J. Chem. Phys. **120**, 5867 (2004).

[32] A. K. Soper and M. A. Ricci, Phys. Rev. Lett., **84**, 2881 (2000).

[33] Th. Strassle, A. M. Saitta, Y. Le. Godec, G. Hamel, S. Klotz, J. S. Loveday, and R. J. Nelmes, Phys. Rev. Lett. **96**, 067801(4pages) (2006).